Available online at www.sciencedirect.com
SCIENCE DIRECT®
Chemical Physics Letters 377 (2003) 340–346
CHEMICAL PHYSICS LETTERS
www.elsevier.com/locate/cplett

Effects of an external electrical field on the polarization of growing organic crystals: a theoretical study

Jürg Hulliger *, Martin Losada, Claire Gervais, Thomas Wüst, Felix Budde

Department of Chemistry and Biochemistry, University of Berne, 3, Freiestrasse, CH-3012 Berne, Switzerland

Received 2 May 2003; in final form 26 June 2003
Published online: 30 July 2003

Abstract

In certain non-ferroelectric molecular crystals a static external electrical field applied during the growth in the high vacuum may induce effects of permanent poling or depoling through interaction with dipolar molecules getting attached to crystal faces. In centrosymmetric crystal structures a field may effect a substantial deviation from a 50%:50% fractional site occupation with respect to the molecular dipole orientation. For channel-type inclusion compounds the electric field may affect growth sectors as such as to annihilate polarity in one sector and to enhance polarity in symmetry related sectors. Numerical simulations are given to show the change in the spatial distribution of polarity, including its temperature dependence.

Reports on the effect of an electrical field on growing crystals describe e.g., nucleation [1] or attempts to influence the orientation of crystallites relative to electrodes [2]. Affecting the *permanent* polarization in molecular crystals is known for a few ferroelectric [3–6] and ferroelastic materials [7,8]. Because of a generally high barrier for a dipole inversion of elongated prolate-top molecules [9] in the crystalline state, a field or stress-induced inversion of individual dipoles in the bulk is not likely for other crystal classes than ferroelectrics or ferroelastics, respectively.

A different case than ferroic materials concerns the application of an external electrical field E during the growth of centrosymmetric or non-centrosymmetric dielectric organic crystals, because at surface sites the activation energy for dipole reversal is much lower than for the bulk. Normally, the energy of attachment for an inverted dipole to a highly ordered structure (molecules aligned into chains, planes, etc) is endothermic. Therefore, defects of this type will show a low probability to occur spontaneously.

Application of a static external field to growing crystals is applied here to centrosymmetric crystals structures, where dipolar molecules on average show a 50%:50% fractional occupation of lattice sites with respect to the orientation of the dipole moments. One of many known example is 4-chloro-4′-nitrostilbene (CNS) crystallizing in $P2_1/c$ [10] (Fig. 1).

* Corresponding author. Fax: +41-31-631-39-93.
E-mail address: juerg.hulliger@iac.unibe.ch (J. Hulliger).

0009-2614/$ - see front matter © 2003 Elsevier B.V. All rights reserved.
doi:10.1016/S0009-2614(03)01128-X

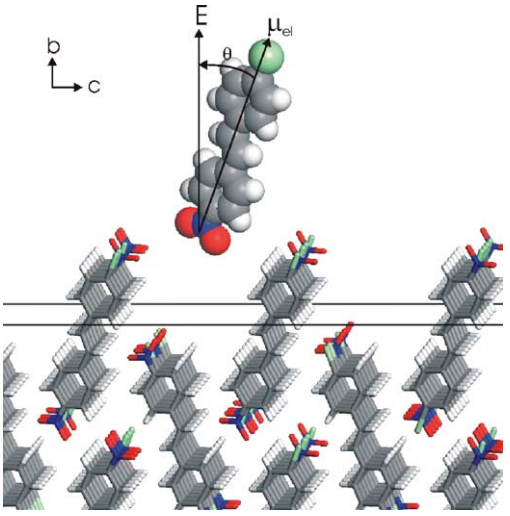

Fig. 1. (0 1 0) face of a CNS crystal showing a 50%:50% orientational disorder between *nitro*-first and *chloro*-first configurations.

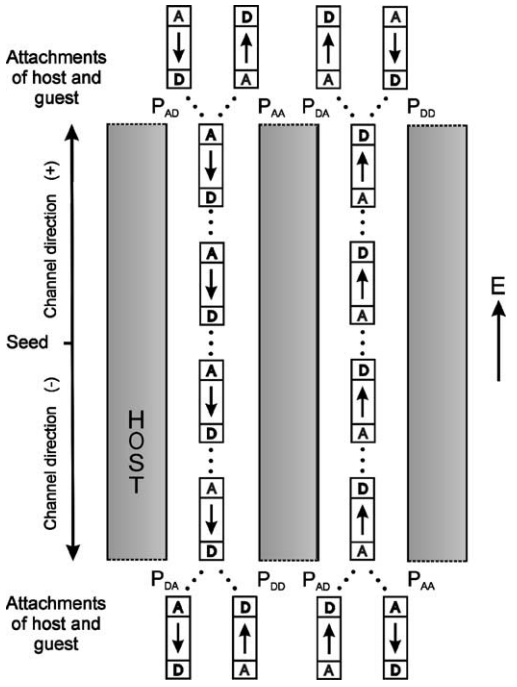

Fig. 2. Schematic view of the attachment of dipolar molecules to growing channels of a channel-type inclusion compound. Molecules A–D may enter by keeping the dipolar orientation as compared to guest molecules in channels or may be attached in the opposite direction. Corresponding attachment probabilities are P_{AD}, P_{AA}, etc. In the case of an applied field E, it is assumed that these probabilities depend also on the applied field. As the channels grow in both directions, corresponding processes take place at each end of channels.

The interaction of the field with the dipole moment of CNS molecules will give rise to a change in the attachment probabilities P_{AD}, P_{AA}, P_{DA} and P_{DD} (A = acceptor-type fragment, here NO_2; D = donor-type fragment, here Cl, see Fig. 2) for entering a crystal face *chloro*-first (D) as compared to *nitro*-first (A). Because of symmetry breaking at the surface [10], attachment probabilities P_{AA} and P_{DD} differ already in the absence of a field. Consequently, some polar alignment of CNS molecules in the crystal structure will take place also in zero field. Phase sensitive second harmonic microscopy was recently able to reveal effects of polarity [11] demonstrating that symmetry related sectors (+)-b and (−)-b feature opposite polarity. As the fraction of parallel aligned dipoles may be as small as a few percent, a structure refinement might not be sensitive enough to account for this type of grown-in stochastic order. The effect of the field will in essence *enhance* or *reduce* the extent of grown-in polarity in CNS crystal sectors as discussed in more details below.

In high vacuum experiments the application of a field E to a growing CNS crystal will effect partial poling: By assuming a field parallel to the b-axis (Fig. 1) and a dipole moment μ_{el}^{CNS} of 3.91 D (The 6-31G(d,p) and 3-21G basis sets were used to obtain the optimized energies and the molecular properties (dipole moment) of CNS and INBP (see below) molecules, respectively. All calculations were carried out with GAUSSIAN 98.), a field strength of about 10^8 V/m (300 K) would be necessary to achieve e.g., an excess (η) of 15.6% of CNS dipoles in the gas phase featuring an angle θ (: μ_{el}, E) smaller than $\pi/2$ ($0 \leqslant \theta(E \neq 0) \leqslant \pi$). Because of a deviation from a random distribution of dipole orientations in the gas phase, we can assume to obtain a similar deviation from 50%:50% in the solid state. Alignment parameters $W(\alpha)$ for the gas phase (Table 1) were calculated by Eq. (1), which was obtained by integrating the angular distribution function $G(\theta, T)$ over the upper hemisphere (Langevin description):

Table 1
Orientational parameter $W(\alpha)$ for different field strengths and CNS molecules in the gas phase

E (V/m)	$T = 300$ K		$T = 250$ K	
	$W(\alpha)$	η (%)[a]	$W(\alpha)$	η (%)[a]
10^6	0.500	0	0.501	0
5×10^6	0.504	0.8	0.505	0.8
10^7	0.508	1.6	0.509	1.7
5×10^7	0.539	7.8	0.547	9.2
10^8	0.578	15.6	0.593	18.4
5×10^8	0.828	65.6	0.868	73.4
10^9	0.958	91.6	0.978	95.2

[a] $\eta = 200\ (W(\alpha) - 0.5)$.

$$W(\alpha) = \frac{1 - e^{\alpha}}{e^{-\alpha} - e^{\alpha}}, \quad \alpha = \frac{N_A \mu_{el} E}{RT}, \tag{1}$$

where $W(\alpha)$ is the fraction of molecules whereof the dipolar moments preferably point into the upper hemisphere (N_A: Avogadro number).

A Markov-type, i.e., stochastic analysis [10] of polarity formation in crystal structures represented by ~50%:50% occupation shows that in the case of a low number of aligned dipoles, the extent of grown-in alignment predominantly depends on *longitudinal* interactions (e.g., E_{AD}, E_{AA}, etc., see Scheme 1) which were attributed to synthon-type intermolecular contacts between the entering functional groups (D, A) and those located on the substrate plane (growing crystal face). This means, CNS may be discussed in the theoretical frame which was developed [12,13] for channel-type inclusion compounds where no *transversal* interactions between guest molecules were assumed for polarity formation.

Along a series of theoretical [12,13] and experimental [14,15] work, we have analyzed a Markov-chain type crystal growth model for grown-in polarity in channel-type inclusion compounds (perhydrotriphenylene, PHTP [15], tris (*o*-phenylenedioxy)cyclotriphosphazene [16]). In these materials, prolate-top dipolar molecules are included into parallel channels being separated by about 10 to 15 Å as to reduce the influence of lateral guest–guest interactions on polarity (Fig. 2). Because of growth in both directions of the channels as well as growth perpendicular to the channels, inclusion crystals show a characteristic inhomogeneous spatial distribution of polarization [17]: Corresponding sectors in the (+)- and (−)-direction of the channels feature an opposite polarization, whereas sectors perpendicular to channels show strong polarization gradients [18]. In Fig. 3 we show a stochastic simulation of the 2D spatial development of down and up orientations of dipoles in sectors labeled $S_{\parallel}^{+}$, $S_{\parallel}^{-}$ and $S_{\perp}$. Nucleation was assumed to occur in the center of the figure. Each square-type pixel represents a molecule in a channel. The average polarity in the sectors $S_{\parallel}^{+}$ and $S_{\parallel}^{-}$ are equal, but different in the sign. As a matter of the co-deposition of host and guest molecules, net polarity in $S_{\perp}$ sectors is smaller than in others.

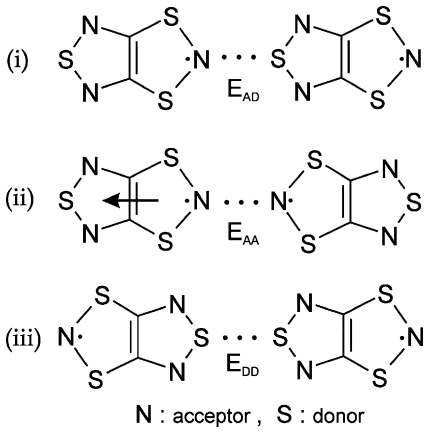

Scheme 1. Molecular structure of the TTTA radical used as a real example here [19]. Outlay of possible -A···D-, -A···A- and -D···D- interactions in a channel-type inclusion compound as e.g., PHTP. These type of collinear interactions are used to calculate attachment probabilities P_{AD}, P_{AA}, etc. Arrow: dipolar moment.

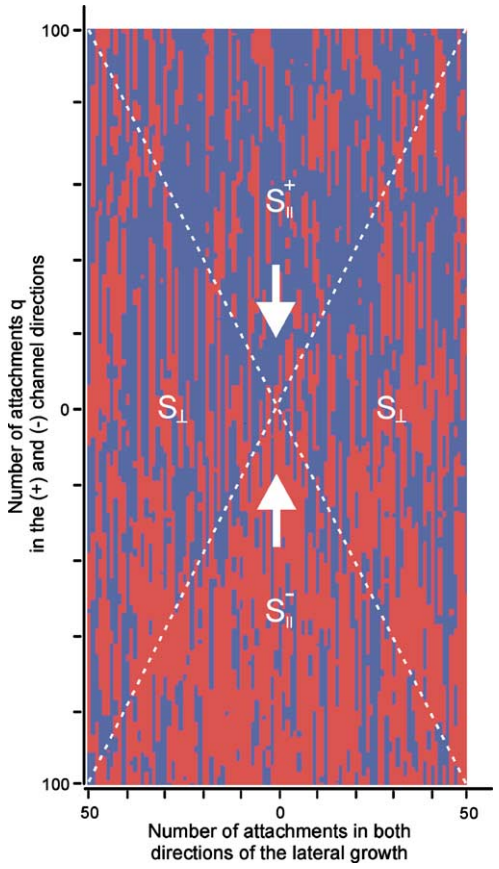

Fig. 3. Stochastic simulation of the development of polarity in 2D. One square pixel corresponds to a guest molecule (black, ↓; grey, ↑; in the electronic version, blue, ↓; red, ↑). In sectors $S_{\parallel}^{\pm}$ we have polarity development of *existing* channels being elongated. In sectors $S_{\perp}$ there is the generation of *new* channels, thus introducing gradients in the distribution of $X_{\text{net}}(y,x)$. Energies used here are: $E_{\text{AD}} = -10$, $E_{\text{AA}} = -1.8$, $E_{\text{DD}} = -3.7$ kJ/mol, $T = 300$ K. White arrows represent average polarity in each sector. For details on the selected example (TTTA), see text. Here $|X_{\text{net}}|$ is 0.34.

In terms of the Markov-chain model [13] attachment probabilities are defined, which drive the vectorial alignment of dipoles entering channels. Probabilities can be calculated using intermolecular interactions energies E_{AD}, E_{AA} and E_{DD} (see Fig. 2 and Scheme 1). To describe the effect of an external field during the process of being attached to a channel-site A-first or D-first, we add here the dipolar energy in the field E to the corresponding attachment energy:

$$\Delta E_{\text{A}}^{\pm} = E_{\text{AA}} - E_{\text{AD}} \mp 2N_{\text{A}}\mu_{\text{el}}E,$$
$$\Delta E_{\text{D}}^{\pm} = E_{\text{DD}} - E_{\text{AD}} \pm 2N_{\text{A}}\mu_{\text{el}}E.$$

In the absence of lateral interactions, ΔE_{A} and ΔE_{D} are the basic energy differences to induce polarity formation.

Provided a large number of attachment steps q have taken place [13], the net fraction X_{net} of vectorial alignment of molecules presenting their A-fragment toward the crystal nutrient interface (Fig. 2) is given by

$$X_{\text{net}}^{\pm} = \frac{1-\varepsilon^{\pm}}{1+\varepsilon^{\pm}}, \tag{2}$$

$$\varepsilon^{\pm} = \frac{1+\mathrm{e}^{\Delta E_{\text{D}}^{\pm}/RT}}{1+\mathrm{e}^{\Delta E_{\text{A}}^{\pm}/RT}}. \tag{3}$$

The + and − sign in Eqs. (2) and (3) and others below refer to either growth in (+)-direction of the channel axis with respect to the field vector E or in the opposite way (−).

In one of the sectors $S_{\parallel}$ the field is thus *opposing* polarity formation, whereas in the opposite sector a field *enhanced* effect will be obtained. For sectors $S_{\perp}$, there is a gradient in the channel direction as well as laterally (Fig. 4). A special situation arises for a field strength where e.g., in sectors $S_{\parallel}^{-}$ there is annihilation of polarity, whereas in $S_{\parallel}^{+}$ maximum polarity is achieved (Fig. 4). From Eq. (3) we obtain the conditions to match the cases where $\epsilon^{\pm}$ reaches unity for a critical field E_{c}:

(i) Growth in direction of the field (+)

$$E_{\text{AA}} - E_{\text{DD}} = 4N_{\text{A}}\mu_{\text{el}}E_{\text{c}}. \tag{4}$$

(ii) Growth in the opposite direction of the field (−)

$$E_{\text{AA}} - E_{\text{DD}} = -4N_{\text{A}}\mu_{\text{el}}E_{\text{c}}. \tag{5}$$

Eqs. (4) and (5) allow to estimate $\Delta E_{\text{A}} - \Delta E_{\text{D}} = E_{\text{AA}} - E_{\text{DD}}$ from growth experiments at a critical field strength E_{c}. As X_{net} depends on ΔE_{A} and ΔE_{D} (Eqs. (2) and (3)), (i) a determination of E_{c} ($X_{\text{net}} = 0$, in e.g., $S_{\parallel}^{-}$) from growth experiments, and (ii) a measurement of X_{net} ($S_{\parallel}$, $E = 0$) from pyroelectric studies [18], would open up a way to obtain basic energy differences driving polarity formation as described by the Markov-chain growth model.

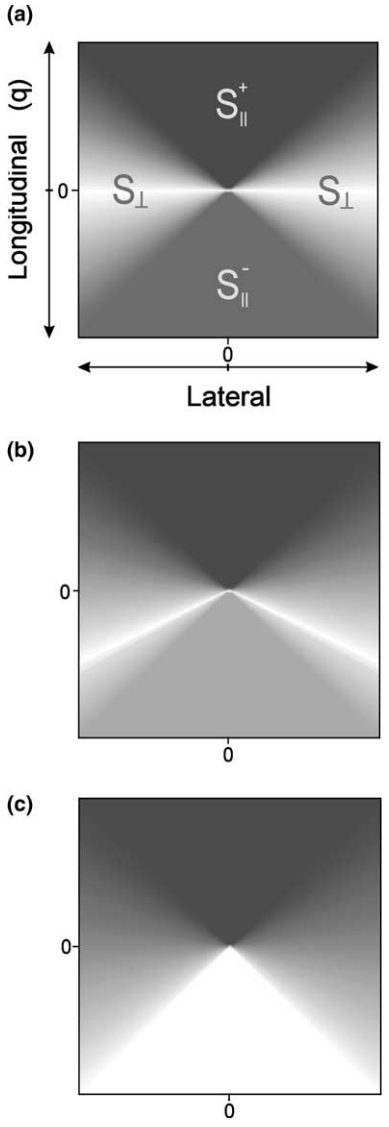

Fig. 4. Polarization distribution by $X_{net}(y,x)$ for different field strengths E at 300 K. Use of Eqs. (6)–(8) allow to calculate the macroscopic distribution for $q = 10^5$ and 10^5 channels in both the + and − lateral direction (dark, strong polarity; white, zero polarity). Seed at (0,0) position. Critical field $E_c = 3.92 \times 10^8$ V/m. (a) $E = 0$, (b) $E = 2 \times 10^8$ V/m, (c) $E = E_c$. With E increasing, the lower sector $S_{\parallel}^{-}$ loses polarity, whereas in the upper one $S_{\parallel}^{+}$ there is an enhancement of X_{net}. For further parameters used here, see text.

To discuss the effect of a field on the molecular alignment by a real example, we use here interaction energies calculated by ab initio quantum mechanical methods for a sulfur–nitrogen radical (TTTA, Scheme 1) included into channels of PHTP: Along chains, TTTA radicals show nitrogen (A) to sulfur (D), nitrogen (A) to nitrogen (A) and sulfur (D) to sulfur (D) interactions mainly effected by terminal atoms ($E_{AD} = -10$, $E_{AA} = -1.8$, $E_{DD} = -3.7$ kJ/mol). Interaction energies were calculated at the CASPT2/cc-pVDZ level of theory using UHF natural orbital occupancies for the determination of the active space (CASSCF(6,6)). For the computation of the dipole moment of a monomer of TTTA, the B3LYP/cc-pVDZ model chemistry was chosen. The calculated dipole moment is 0.61 D. In the upper sector of Figs. 4b and c there is an *increase*, in the lower one a *reduction* of net polarity for fields in the range of e.g., 2–3.92×10^8 V/m.

The spatial distribution (y, channel direction; x, lateral) of X_{net} (y,x) was calculated by assuming (i) growth along existing channels, and (ii) generation of new channels in the lateral direction [17]. Starting from a seed at $y = x = 0$, two basically different types of sectors are formed (see Fig. 3 for definition): Sectors $S_{\parallel}^{+}$ and $S_{\parallel}^{-}$, where a rather homogeneous average polarity X_{net} is obtained, and sectors $S_{\perp}$ where gradients appear. At a field strength E_c of 3.92×10^8 V/m (Fig. 4c), here net polarity in the lower sector becomes zero.

For a system showing constant X_{net} values ($S_{\parallel}^{\pm}$) after a low number of attachment steps q as compared to the size of a real crystal, X_{net} (y,x) can be described by three simplified equations:

(i) Sectors $S_{\parallel}^{\pm}$

$$X_{net}^{+}(y,x) = X_{net}^{+}, \tag{6}$$

$$X_{net}^{-}(y,x) = X_{net}^{-}. \tag{7}$$

(ii) Sectors $S_{\perp}$

$$X_{net}(y,x) = \frac{X_{net}^{+} - X_{net}^{-}}{2v}\,\frac{y}{|x|} + \frac{X_{net}^{+} + X_{net}^{-}}{2}, \tag{8}$$

where v is the ratio of the growth speeds with respect to the y and x direction.

The case of the radical inclusion is of special interest here, because we can make use of the interplay between polarity formation in individual channels and the setting up of magnetically coupled chains of radicals in channels (for details on

this particular issue, see reference [19]): By a Markov-chain mechanism, average chain lengths L_A and L_D of interacting radicals [20] are formed which in zero field are 28 and 14, respectively (300 K) [19]. Application of an E field can bring in a significant change:

$$L_A^{\pm} = \frac{1}{P_{AA}^{\pm}}, \qquad L_D^{\pm} = \frac{1}{P_{DD}^{\pm}}, \tag{9}$$

where

$$\frac{1}{P_{AA}^{\pm}} = 1 + e^{\Delta E_A^{\pm}/RT}, \tag{10}$$

$$\frac{1}{P_{DD}^{\pm}} = 1 + e^{\Delta E_D^{\pm}/RT}. \tag{11}$$

From Eqs. (10) and (11) we obtain E_c to calculate $L_A = L_D = 19$ ($E_c \approx 3.92 \times 10^8$ V/m). Application of E_c thus allows to have an external influence on the formation of magnetically coupled chains. Because of $L_A = L_D$, a comparison between an experimental and theoretical analysis of magnetic interactions will be facilitated.

Obviously, the extent of thermal fluctuation has a strong influence on the ordering driven by given interaction energies E_{AD}, E_{AA}, etc. and the field. Lowering the growth temperature is hence of interest to reduce the necessary field strength to obtain significant changes in the polarity in real experiments. To demonstrate the effect of the growth temperature, we use another example for a guest molecule to include into channels of PHTP: 4-iodo-4′-nitrobiphenyl (INBP) [21]. Interaction energies (kJ/mol) $E_{AD} = -5.7$, $E_{DD} = -2.8$ and $E_{AA} \approx 10$ (E_{AA} calculated for a van der Waals distance of 3.4 Å) were obtained by application of the Dreiding 2.2.1 force field [22] (calculations were performed using the cerius2 software, Molecular simulations, Cambridge, UK). The calculated dipole moment is 4.26 D. In Fig. 5 we show the influence of the growth temperature for different fields E: In sectors $S_{\parallel}^{+}$ as compared to $S_{\parallel}^{-}$ differences in X_{net} are more pronounced at *low* temperature, because of more steps q needed to achieve asymptotic values for X_{net}.

In summary, we have discussed realistic effects of an applied external field during the growth of organic crystals which allow for a poling or depoling of non-ferroelectric materials. In the frame of a Markov-type description of polarity formation, single component molecular crystals featuring a near to 50%:50% orientational disorder of their dipolar direction and channel-type inclusion compounds are expected to show a similar behavior, although the crystal architecture of corresponding materials is very different.

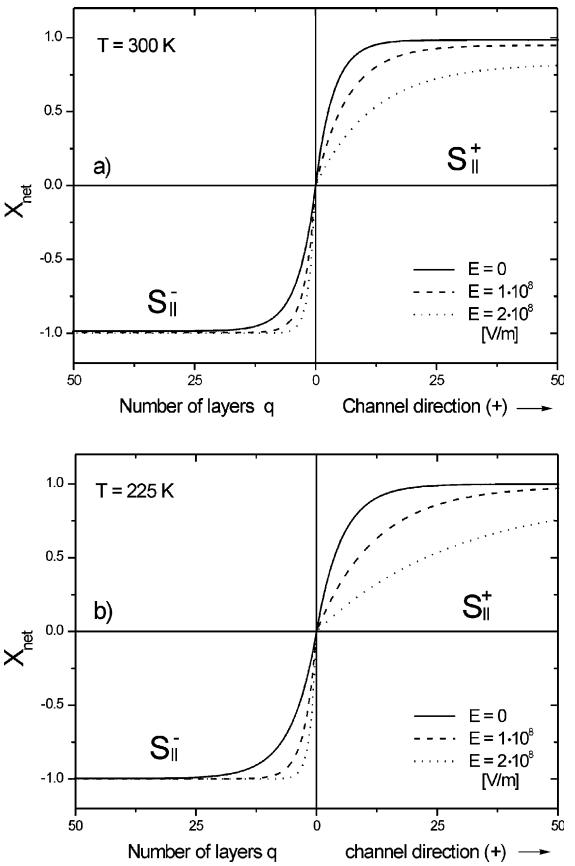

Fig. 5. Effect of temperature on X_{net} for sectors $S_{\parallel}^{\pm}$. Energy parameters are taken for IBNP, see text. The field makes convergence to a constant value of X_{net} more effective in $S_{\parallel}^{-}$ as compared to $S_{\parallel}^{+}$.

Acknowledgements

The work has received support from the Swiss National Science Foundation. Project no. 2000-063777.

References

[1] E.M. da Silva Marques Nogueira, E. de Matos Gomes, M.S. Besley, S. Lanceros-Méndez, J.M. Cerqueira Cunha, A.C. Vega, J.F.C. da Luz Mano, Solid State Sci. 3 (2001) 733–740.
[2] C.Y. Liu, V. Lynch, A.J. Bard, Chem. Mater. 9 (1997) 943.
[3] J. Fousek, Ferroelectrics 113 (1991) 3.
[4] J. Dolinšek, D. Arčon, Hae Jin Kim, J. Seliger, V. Žagar, P. Vaněk, J. Kroupa, Z. Zikmund, J. Petzelt, Phys. Rev. B 57 (1998) 8063.
[5] M. Kunimoto, R. Etoh, T. Hayashi, T. Kohmoto, Y. Fukada, M. Hashimoto, J. Phys. Soc. Jpn. 71 (2002) 955.
[6] G. Arunmozhi, E.de.M. Gomes, J.L. Ribeiro, Phys. B 325 (2003) 26–34.
[7] N. Morita, H. Nakayama, K. Ishii, J. Phys. Soc. Jpn. 60 (1991) 2684.
[8] L. Rubio-Pena, T. Breczewski, E.H. Bocanegra, Ferroeletrics 269 (2002) 1019.
[9] H. Serrano-González, K.D.M. Harris, S.J. Kitchin, A. Alvarez-Larena, E. Estop, X. Alcobé, E. Tauler, M. Labrador, D.C. Apperley, J. Solid State Chem. 143 (1999) 285.
[10] J. Hulliger, H. Bebie, S. Kluge, A. Quintel, Chem. Mater. 14 (2002) 1523.
[11] S. Kluge, F. Budde, I. Dohnke, P. Rechsteiner, J. Hulliger, Appl. Phys. Lett. 81 (2002) 247.
[12] J. Hulliger, P. Rogin, A. Quintel, P. Rechsteiner, O. König, M. Wübbenhorst, Adv. Mater. 9 (1997) 677.
[13] J. Hulliger, P.J. Langley, O. König, S.W. Roth, A. Quintel, P. Rechsteiner, Pure Appl. Opt. 7 (1998) 221.
[14] J. Hulliger, O. König, R. Hoss, Adv. Mater. 7 (1995) 719.
[15] R. Hoss, O. König, V. Kramer-Hoss, U. Berger, P. Rogin, J. Hulliger, Angew. Chem. Int. Ed. Engl. 35 (1996) 1664.
[16] T. Hertzsch, S. Kluge, E. Weber, F. Budde, J. Hulliger, Adv. Mater. 13 (2001) 1864.
[17] J. Hulliger, A. Quintel, M. Wübbenhorst, P.J. Langley, S.W. Roth, P. Rechsteiner, Opt. Mater. 9 (1998) 259.
[18] A. Quintel, S.W. Roth, J. Hulliger, M. Wübbenhorst, Mol. Cryst. Liq. Cryst. A 338 (2000) 243.
[19] H.I. Süss, T. Wüst, A. Sieber, R. Althaus, F. Budde, H.-P. Lüthi, G.D. McManus, J. Rawson, J. Hulliger, Cryst. Eng. Commun. 4 (2002) 432.
[20] A. Quintel, J. Hulliger, Chem. Phys. Lett. 312 (1999) 567.
[21] J. Hulliger, P.J. Langley, Chem. Commun. (1998) 2557.
[22] S.L. Mayo, B.D. Olafson, W.A. Goddard III, J. Phys. Chem. 94 (1990) 8897.